Supplementary Information for

Dissecting the role of inter-protomer cooperativity in the activation of oligomeric high temperature requirement A2 protein

This PDF file includes:

Supplementary text

Figures S1 to S8

SI References

SI Text

Inter-protomer allostery

In this manuscript we demonstrate that HtrA2 function is regulated, in part, through an inter-protomer allosteric network that communicates binding of PDZ- and substrate peptides at a given protomer to neighboring subunits. We have interpreted the allostery focusing on a trimeric HtrA2 structure, but it is important to emphasize that (i) apo-HtrA2 exchanges between trimeric and hexameric states and that both salt and high temperature shift the equilibrium to the hexamer and (ii) that there is a second trimer-hexamer equilibrium for the PDZ-ligated particles as well (1). Several lines of evidence point to the fact that the trimer is the "allosteric unit". First, the trimeric structure has a much higher affinity for PDZ-peptide (*i.e.*, a mimic for the C-terminal region of substrate molecules), so that the interaction between PDZ-peptide and HtrA2 occurs at the level of trimers, as established previously (1).

Thus, the increase in PDZ-peptide affinity with binding occupancy reflects inter-subunit cooperativity within the context of a trimer (Fig. 1). Second, our enzyme assays (Fig. 4) are performed using a protein concentration of 100 nM (subunit concentration) so that HtrA2 would be predominantly trimeric. Prominent inter-subunit allosteric effects are observed in this assay, whereby only the fully open PDZ-peptide engaged state is active, again consistent with a trimer as the basic allosteric unit. (iii) Notably, NMR spectra of HtrA2 with PDZ-peptide *and* substrate were recorded at 200 mM NaCl (as opposed to 0 mM added salt for the other NMR experiments) to solubilize the substrate-bound complex. At this concentration of salt and at 40 ^{o}C a large fraction of HtrA2 exists in the hexameric state (*SI Appendix*, Fig. S7E). Although chemical shift differences between trimeric and hexameric structures are, in general, very small (1), our data indicate that the hexameric state predominates under these conditions. The NMR results showing that structural changes upon substrate binding can only be accommodated in a symmetric sample where all protomers (hexamer) are wild-type (Fig. 5) is consistent with results from the peptidase assays (trimer), suggesting that the same allosteric network is operative in both classes of HtrA2 oligomer. Throughout the paper we have chosen to represent HtrA2 schematically as a trimer for simplicity, but in cases of high salt (200 mM) and temperature (40 ^{o}C) the hexamer dominates. Nevertheless, the exact nature of the oligomeric state does not affect any of our conclusions.

Signal splitting observed in mixed samples

As described in the text we have probed allostery in the HtrA2 homo-oligomeric system through studies of molecules that were engineered by mixing different types of protomers. As such there is a statistical distribution of configurations that are produced (denoted by A-D in Fig. 2A) and under the conditions of our mixing experiments only configurations B and C are NMR observable. For example,

in an asymmetric sample prepared by mixing 90% U-^{2}H E425C PDZ-peptide stapled/open protomers and 10% U-^{2}H, *proR* ILVM-$^{13}CH_3$ native protomers a pair of NMR observable molecules are produced, corresponding to one native protomer/two PDZ-stapled protomers (configuration B) and two native protomers/one PDZ-stapled protomer (configuration C) (Fig. 3A & *SI Appendix* Fig. S4A, schematic of asymmetric trimers). Although there is a 9:1 ratio in populations (B:C), the NMR signal derived from B and C is in a 9:2 ratio, as configuration C is comprised of two NMR active protomers, while configuration B has only a single such subunit. We wondered if it might be possible to see separate signals from configurations B and C, therefore. For the majority of methyl probes separate crosspeaks corresponding to configurations B and C could not be observed. However, for a number of methyl groups, L173, I179, V199, and V396, a pair of peaks was indeed noted, with an approximate intensity ratio of 9:2 (*SI Appendix* Fig. S4A, green). These methyls are attached to residues located at the intra-protomer protease-PDZ domain interface that we have shown is sensitive to the open/closed conformation of adjacent subunits (see *text*). The major crosspeak derived from each pair, assigned to configuration B, is located at a position distinct from the corresponding peak in spectra of the symmetric closed state, while the minor peaks (configuration C) appear to be essentially degenerate with the correlations from symmetric closed particles. In contrast, I150 and I234, located near the inter-protomer trimer interface, did not show splitting of methyl group signals, although their chemical shifts were significantly different than those derived from the symmetric closed protomer. Thus, configurations B and C may differ structurally in the protease-PDZ domain interface (intra-subunit), while sharing similar structural features in the interface connecting protease domains from neighboring subunits.

Materials and methods

Protein expression and purification

The codon-optimized human S306A HtrA2 gene (residues 134-458 Uniprot: O43464) was synthesized by GenScript and cloned into a pET-SUMO vector as previously described (1). All HtrA2 mutations were introduced by using Quikchange site-directed mutagenesis (Agilent). For producing non-labeled proteins, transformed *E. coli* BL21(DE3) cells were grown in LB media at 37 °C. Cells were induced by adding 0.2 mM isopropyl β-D-1-thiogalactopyranoside (IPTG) at an OD_{600} of ~0.7 and grown for ~18 hours at 25 °C. For producing isotopically-labeled proteins, transformed *E. coli* BL21(DE3) cells were grown in minimal M9 D_2O media supplemented with d_7-glucose as the sole carbon source along with the addition of precursors (60 mg/L 2-keto-3-d_2-4-^{13}C-butyrate for Ileδ1-$^{13}CH_3$, 60 mg/L 2-keto-3,3,4,4-d_4-4-^{13}C-butyrate for Ileδ1-$^{13}CHD_2$, 80 mg/L 2-keto-3-methyl-d_3-3-d_1-4-^{13}C-butyrate for Leu,Val-$^{13}CH_3$/$^{12}CD_3$ non-stereospecific isopropyl methyls, 230 mg/L 2-hydroxy-2-methyl-d_3-3-oxobutanoate-4-^{13}C for Leuδ1,Valγ1-$^{13}CH_3$, *proR* stereospecific isopropyl labeling, and 100 mg/L methyl-$^{13}CH_3$-methionine for Metε) 1 hour prior to induction of protein overexpression (2, 3). Cells were induced by adding 0.2 mM IPTG at an OD_{600} of ~0.7 and grown for ~18 hours at 25 °C. Proteins were purified by Ni-affinity chromatography using a 5 mL HisTrap HP column (Cytiva) or HIS-Select Nickel Affinity Gel (Sigma) and eluted in buffer containing 20 mM HEPES-NaOH (pH 7.4), 300 mM NaCl, 300 mM imidazole. The N-terminal His_6-SUMO tag was cleaved by the addition of Ulp1 protease. Protein purification was further achieved by hydrophobic interaction chromatography with a HiTrap Butyl HP column (Cytiva) using a buffer-gradient of 20 mM HEPES-NaOH (pH 7.4), 0-500 mM $(NH_4)_2SO_4$, 1 mM EDTA. The eluted fractions containing full-length proteins were concentrated by using an Amicon Ultra-15 30K MWCO concentrator and subjected to size exclusion chromatography on a Superdex 200 Increase column (Cytiva) in buffer

containing 20 mM HEPES-NaOH (pH 7.4), 300 mM NaCl, 1 mM EDTA. His_6-SUMO-tagged proteins for establishing random protomer mixing (*SI Appendix*, Fig. S2) were purified by Ni-affinity chromatography and then directly subjected to size exclusion chromatography without His_6-SUMO tag cleavage. Protein concentrations were measured based on molar extinction coefficients at 280 nm (8,940 M^{-1} cm^{-1} for V226C/Y428C/S306A and V226C/Y428C/S306A/I441V mutants in the reduced form, 10,430 M^{-1} cm^{-1} for the wild-type protein and other mutants, and 11,920 M^{-1} cm^{-1} for the His_6-SUMO-tagged S306A/I441V mutant). PDZ-peptide (DDGQYYFV) and the substrate peptide (IRRVSYSFKKK) were synthesized by Genscript. Peptide concentrations were measured based on molar extinction coefficients at 280 nm (2,980 M^{-1} cm^{-1} for PDZ-peptide and 1,490 M^{-1} cm^{-1} for the substrate).

Cysteine cross-linking reaction

To prepare the N-terminally modified PDZ-peptide to generate stapled protomers (Fig. 1B), 1 mM PDZ-peptide and 5 mM *N*-succinimidyl 3-(2-pyridyldithio) propionate (SPDP) (Sigma-Aldrich) (from 20 mM DMSO stock) were incubated at 37 °C for 2 hours in buffer containing 20 mM HEPES-NaOH (pH 7.4) and 1 mM EDTA. The N-terminally modified PDZ-peptide was purified by anionic exchange chromatography with a Hitrap Q XL 1 mL (Cytiva) column using a gradient of 20 mM - 1 M NH_4HCO_3. The modified PDZ-peptide concentration was estimated based on a molar extinction coefficient at 280 nm of 8,080 M^{-1} cm^{-1} (4). E425C/S306A/I441V mutant HtrA2 (to which the PDZ-peptide was stapled) was buffer exchanged into a DTT-free buffer (20 mM HEPES-NaOH (pH 7.4) and 1 mM EDTA) and concentrated to 50-200 μM. Then, 1.5-2 equimolar N-terminally modified PDZ-peptide was directly added to the solution and incubated at 37 °C for 1 hr. The completion of the

reaction was confirmed by monitoring the release of pyridine-2-thione, using the absorbance at 340 nm (molar extinction coefficient of 8,080 M^{-1} cm^{-1}), and nearly 100% modification was achieved in all cases. The modification of the PDZ-peptide was also confirmed by electrospray ionization mass spectrometry. To generate the disulfide bond between the PDZ and protease domains of HtrA2 protomers ("locked" state), symmetric or mixed forms of HtrA2 containing purified V226C/Y428C/S306A or V226C/Y428C/S306A/I441V protomers were concentrated to ~20 μM in an Amicon Ultra-15 30K MWCO concentrator and subsequently incubated at 37 °C overnight in the presence of 100 μM copper-1,10-phenanthroline (5). After either of the two Cys-modifying reactions described above, proteins were further purified by size exclusion chromatography on a Superdex 200 Increase column (Cytiva) to remove excess N-terminally modified PDZ-peptide (stapled sample) or copper-1,10-phenanthroline (locked sample).

Preparation of mixed proteins

To prepare mixed HtrA2 protein samples comprised of different types of protomers (Fig. 2A, 4A and *SI Appendix*, Fig. S2A), purified symmetric HtrA2 proteins, containing all wild-type or all mutant/modified protomers, were mixed at the desired ratio using a total protomer concentration of 40 μM in a buffer (for example, 36 μM NMR invisible, 4 μM NMR visible subunits) containing 20 mM HEPES-NaOH (pH 7.4), 300 mM NaCl, 6 M guanidinium chloride, 1 mM EDTA. 1 mM DTT was added when Cys mutant protomers were used. The mixture was then refolded via 15-fold fast dilution into the same buffer without guanidinium chloride. The symmetric sample used for control experiments was also refolded by the same procedure. When Cys mutant subunits were involved the attachment of the PDZ-peptide or the formation of the inter-domain disulfide bond was performed after refolding, as

described above. The mixed proteins were subsequently purified by size exclusion chromatography on a Superdex 200 10/300 Increase column (Cytiva) in buffer containing 20 mM HEPES-NaOH (pH 7.4), 300 mM NaCl, 1 mM EDTA. When mixed proteins comprising S306A/I441V protomers and PDZ-peptide stapled E425C/S306A/I441V protomers were generated, a further purification step was employed involving hydrophobic interaction chromatography with a HiTrap Butyl HP column (Cytiva) using a buffer-gradient of 20 mM HEPES-NaOH (pH 7.4), 0-500 mM $(NH_4)_2SO_4$, 1 mM EDTA, to completely remove any free PDZ-peptide.

NMR experiments

All NMR measurements were performed at 23.5 Tesla (1 GHz ^{1}H frequency) on a Bruker Avance Neo spectrometer or at 14.0 Tesla (600 MHz ^{1}H frequency) on a Bruker Avance III HD spectrometer, equipped with cryogenically cooled *x*, *y*, *z* pulsed-field gradient triple-resonance probes. All measurements were performed at 40 °C unless indicated otherwise. HtrA2 sample concentrations ranged from 50 – 200 μM (monomer concentration), in an NMR buffer consisting of 20 mM HEPES-NaOH (pD 7.4), with or without 200 mM NaCl, 1 mM EDTA, 100% D_2O. 5 mM DTT was added to the buffer for experiments performed under reducing conditions. ^{13}C-^{1}H HMQC spectra that exploit the methyl-TROSY effect were recorded as described previously (6, 7). 200 mM NaCl was added in the experiments observing the interaction with the substrate peptide, as substrate-bound HtrA2 proteins were not stable at low salt concentrations, probably due to an altered surface charge distribution in the substrate-bound state. All spectra were processed and analyzed using the *NMRPipe* suite of programs (8) and visualized using the Python package *nmrglue* (9). Peak intensities were extracted either by using the Peakipy software package (https://github.com/j-brady/peakipy) or by box-sum

integration using an in-house Python script. The methyl signal assignments were transferred from a previous study (1).

The PDZ-peptide titration experiments (Fig. 2C) were measured at a static magnetic field of 14.0 Tesla (600 MHz ^{1}H frequency) using: (1) a 200 μM (monomer concentration) mixed sample comprised of 90% U-^{2}H, Met-$^{13}CH_3$ V226C/Y428C/S306A/I441V (oxidized) and 10% U-^{2}H, *proR* ILV-labeled S306A/I441V, and (2) a 200 μM (monomer) mixed sample comprising 90% U-^{2}H Met-$^{13}CH_3$ PDZ-peptide stapled E425C/S306A/I441V and 10% U-^{2}H, *proR* ILV-labeled S306A/I441V protomers. The PDZ-peptide concentrations used in the titration of Sample 1 were 0, 75, 170, 286, 564, 936, 1210, and 1500 μM; and 0, 20, 52, 115, 196, 304, and 500 μM for the titration of Sample 2. Free and bound crosspeaks derived from I164, L232, I274, I362, and L377 methyl groups in Sample 1 were selected for analysis, while those from I164, L232, and I362 were used for fitting in Sample 2; I274 and L377 were not selected as these signals were severely broadened in spectra of Sample 2. Titration data for these peaks were globally fit using the 2D lineshape fitting program *TITAN* (10) using the standard HMQC scheme, through the *NMRbox* platform (11). Errors in the association constants were obtained through a boot-strap analysis built into *TITAN*.

An HMQC based 2D NOESY experiment recording the ^{13}C chemical shift of the origination methyl and the ^{1}H shift of the destination methyl (^{1}H-^{13}C[t_1]-*mix*-^{1}H[t_2]) was measured at a static magnetic field of 14.0 Tesla (600 MHz ^{1}H frequency), using a 150 μM (monomer concentration) U-^{2}H, *proR* ILVM-labeled S306A/I441V sample and a 250 μM (monomer concentration) mixed sample comprised of 90% U-^{2}H PDZ-peptide stapled E425C/S306A/I441V and 10% U-^{2}H, *proR* ILVM-labeled S306A/I441V protomers (Fig. 3B). A mixing time of 200 ms was used.

^{13}C-^{1}H multiple-quantum Carr-Purcell-Meiboom-Gill (CPMG) relaxation dispersion experiments were performed with a pulse scheme described previously (12) at a static magnetic field of 14.0 Tesla (600 MHz ^{1}H frequency), using a 150 μM (monomer) U-^{2}H, *proR* ILVM-labeled S306A/I441V sample and a 250 μM (monomer) mixed sample consisting of 90% U-^{2}H PDZ-peptide stapled E425C/S306A/I441V and 10% U-^{2}H, *proR* ILVM-labeled S306A/I441V protomers. Two CPMG fields of 66 Hz and 2 kHz were used with a constant-time relaxation delay of 15 ms.

Peak assignments of the active HtrA2 conformation were obtained via magnetization exchange (13), connecting resonances from HtrA2 with and without peptide bound in the active site (*SI Appendix*, Fig. S7C). A set of 3D ^{1}H-^{13}C[t_1]-*mix*-^{13}C[t_2]-^{1}H[t_3]/^{1}H[t_1]-*mix*-^{13}C[t_2]-^{1}H[t_3] magnetization exchange experiments were measured at a static magnetic field strength of 23.5 Tesla and 40 °C, or at 14.0 Tesla and 50 °C. Sequences were modified based on the ^{13}C-CEST experiment used to observe side-chain CHD_2 groups (14). A 200 μM (monomer concentration) U-^{2}H, Ile-$^{13}CHD_2$ S306A/I441V sample containing 4 mM PDZ-peptide was used. Under these experimental conditions, the PDZ-peptide is fully bound to each PDZ domain of the trimer and, additionally, fractionally bound to the substrate binding site of the protease domain, with populations of the open-inactive and active conformations of ~0.4 and ~0.6, respectively. A mixing time of 900 ms was used.

Quantification of substrate peptide affinity

The affinity of an 11-residue substrate peptide (IRRVSYSFKKK) was established by monitoring volumes of peaks in HMQC spectra derived from a sample of the open state of HtrA2 containing excess of PDZ-peptide (100 μM HtrA2, 1 mM PDZ-peptide). Separate sets of peaks were observed throughout the course of the titration, corresponding to substrate free and bound conformers

with correlations from I150 (free and bound signals) and I274 (only the bound signal) used in the analysis. As mentioned in the main text, at the concentrations of PDZ-peptide used to ensure an open HtrA2 conformation that is required for substrate peptide binding there is some residual binding of the PDZ-peptide to the substrate-binding site (Fig. 5, *SI Appendix* Fig. S7). For example, close inspection of Fig. 5A (left) shows major and minor peaks for I150 in the 100 μM HtrA2, 1 mM PDZ-peptide sample (*i.e.*, prior to the addition of substrate). The minor peak is at the position of the substrate bound form of the enzyme and thus reflects a small, but non-zero affinity of the PDZ-peptide for the substrate binding site. As a result we fit the disappearance of free state peaks and appearance of bound correlations to a model in which both substrate and PDZ-peptides compete for the same site, with separate affinities. We have used a very simple competitive binding model which assumes that binding to the substrate site occurs with no cooperativity. Here we define two association constants for the substrate and PDZ-peptides, K_{sub} and K_{pdz}, respectively.

$$\begin{aligned} P + L_{sub} &\rightleftarrows PL_{sub} \qquad K_{sub} = \frac{[PL_{sub}]}{[P][L_{sub}]} \\ P + L_{pdz} &\rightleftarrows PL_{pdz} \qquad K_{pdz} = \frac{[PL_{pdz}]}{[P][L_{pdz}]} \end{aligned} \qquad [1]$$

where P, L_{sub}, L_{pdz} denote an HtrA2 protomer, the substrate peptide, and the PDZ-peptide, respectively. The total HtrA2 protomer (C_{T}) and peptide ($L_{\text{sub,tot}}$ for the substrate peptide and $L_{\text{pdz,tot}}$ for PDZ-peptide) concentrations are defined as follows,

$$\begin{aligned} C_T &= [P] + [PL_{sub}] + [PL_{pdz}] \\ L_{sub,tot} &= [L_{sub}] + [PL_{sub}] \\ L_{pdz,tot} &= [L_{pdz}] + [PL_{pdz}] \end{aligned} \qquad [2]$$

where C_T = 100 μM, $L_{\text{pdz,tot}}$ = 900 μM assuming that 100 μM out of the 1 mM added PDZ-peptide binds

tightly to the PDZ domain of HtrA2, and $L_{sub,tot}$ was varied from 0 to 2000 μM. The NMR signal intensities for the free (I_{free}) and bound (I_{bound}) states were calculated by converting the molar concentration terms into fractional populations using the following equations.

$$I_{free} \propto \frac{[P]}{C_T}$$
$$I_{bound} \propto \frac{([PL_{sub}] + [PL_{pdz}])}{C_T} \quad [3]$$

The optimal values of K_{sub} and K_{pdz} were obtained by computing I_{free} and I_{bound} values according to Eqs. 1-3 and minimizing the residual sum-of-squared (RSS) differences between them and the corresponding experimental NMR signal intensities according to

$$RSS = \sum_{j} \sum_{i-1}^{N} \left(I_{j,i}^{exp.}(L_{sub.tot,i}) - I_{j,i}^{sim.}(L_{sub.tot,i}) \right)^2 \quad [4]$$

where $j \in \{free, bound\}$, $I_{j,i}^{exp.}(L_{sub.tot,i})$, and $I_{j,i}^{sim.}(L_{sub.tot,i})$ are the experimental and fitted data respectively, Minimization of the above target function was achieved using in-house written programs (Python 3.7), exploiting the Nelder-Mead algorithm of the Lmfit python software package (https://lmfit.github.io/lmfit-py/). The K_{sub} and K_{pdz} were calculated to be 3.5 $\pm$ 0.5 × 10^3 (M^{-1}) and 3.7 ± 0.8 × 10^2 (M^{-1}), respectively.

Peptidase assay

The HtrA2 peptidase activity was measured at 40 °C using the peptide Mca-IRRVSYSF{Lys(Dnp)}KK (Dnp: N-dinitrophenyldiaminopropionic acid) (GenScript) as substrate, in which a fluorogenic 7-methoxy-coumarin-4-acetic acid (Mca) group was attached to the N-terminus (1, 15) (Fig. 4). The reaction was monitored with a Synergy Neo2 96-well microplate reader every 21

seconds using λ_{ex}: 320 nm, λ_{em}: 390 nm with 10 nm bandwidths. Measurements were conducted with 100 nM mixed HtrA2 samples, comprised of U-^{2}H wild-type and U-^{2}H V226C/Y428C/S306A (oxidized) protomers at various ratios, 10 μM substrate peptide and 1 mM PDZ-peptide dissolved in buffer containing 20 mM HEPES-NaOH (pD 7.4), 200 mM NaCl, 1 mM EDTA, D_2O. For the experiments recorded under reducing condition, the proteins were reduced by incubating with 5 mM DTT for 10 minutes at 37 °C, and 5 mM DTT was added to the assay buffer. Catalytic rates were generated from the initial slope of activity *vs* time profiles and normalized by the rate corresponding to the wild-type, fully active and symmetric form of HtrA2 (Fig. 4B, left). Error bars in Figure 4B (left) correspond to one standard deviation based on triplicate measurements.

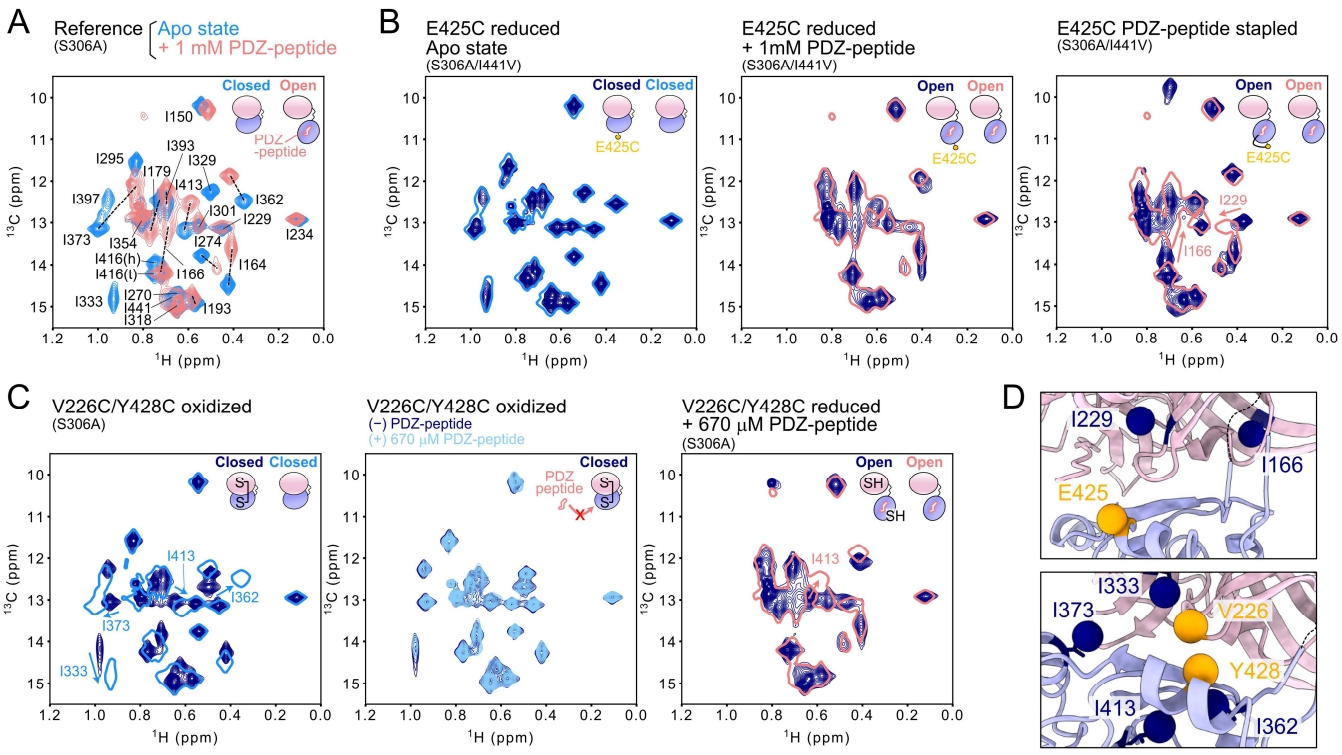

Figure S1. NMR spectra of HtrA2 Cys mutants. (A) ^{13}C-^{1}H HMQC spectra of U-^{2}H, *proR* ILVM S306A HtrA2 in the absence (blue) and presence (pink) of 1 mM PDZ-peptide. (B) (*left*) ^{13}C-^{1}H HMQC spectrum of U-^{2}H, *proR* ILVM E425C/S306A/I441V HtrA2 under reducing conditions. The spectrum of the U-^{2}H, ILVM S306A/I441V HtrA2 is shown in light blue, single contours. PDZ-peptide was not added. (*center*) ^{13}C-^{1}H HMQC spectrum of U-^{2}H, *proR* ILVM E425C/S306A/I441V HtrA2 in the presence of 1 mM PDZ-peptide under reducing conditions (navy). The spectrum of U-^{2}H, ILVM S306A/I441V HtrA2 in the presence of 1 mM PDZ-peptide is shown as pink single contours. (*right*) ^{13}C-^{1}H HMQC spectrum of U-^{2}H, *proR* ILVM E425C/S306A/I441V PDZ-peptide stapled HtrA2 (navy). The spectrum of U-^{2}H, ILVM S306A/I441V HtrA2 in the presence of 1 mM PDZ-peptide is shown with pink single contours. (C) (*left*) ^{13}C-^{1}H HMQC spectrum of U-^{2}H, *proR* ILVM V226C/Y428C/S306A under oxidizing conditions (navy). The spectrum of the U-^{2}H, *proR* ILVM S306A HtrA2 is shown with blue single contours. PDZ-peptide was not added. (*center*) Superposition of ^{13}C-^{1}H HMQC spectra of U-^{2}H, *proR* ILVM V226C/Y428C/S306A in absence (navy) and in the presence of 670 µM PDZ-peptide (cyan) under oxidizing conditions. (*right*) ^{13}C-^{1}H HMQC spectrum of U-^{2}H, *proR* ILVM V226C/Y428C/S306A HtrA2 under reducing condition in the presence of 670 µM PDZ-peptide (navy). The spectrum of U-^{2}H, *proR* ILVM S306A HtrA2 in the presence of 1 mM PDZ-peptide is shown with

pink single contours. (D) Methyl reporters with significant chemical shift differences in superimposed spectra in panels B and C are highlighted with navy spheres, and Cβ carbons of mutated residues to generate Cys are indicated by orange spheres, both mapped onto an HtrA2 protomer (PDB ID: 1LCY) (top panel: E425C mutant, bottom panel: V226C/Y428C mutant). The mapping reveals that residues with perturbed methyl chemical shifts are in close proximity to the modification sites. All NMR data sets were recorded at 23.5 Tesla and 40 °C. Schematics of HtrA2 protomeric structures used in the spectral comparisons are shown in the top right of the spectra. Many of the spectra highlighted are as per Figure 1 of the main text, but with larger chemical shift regions plotted.

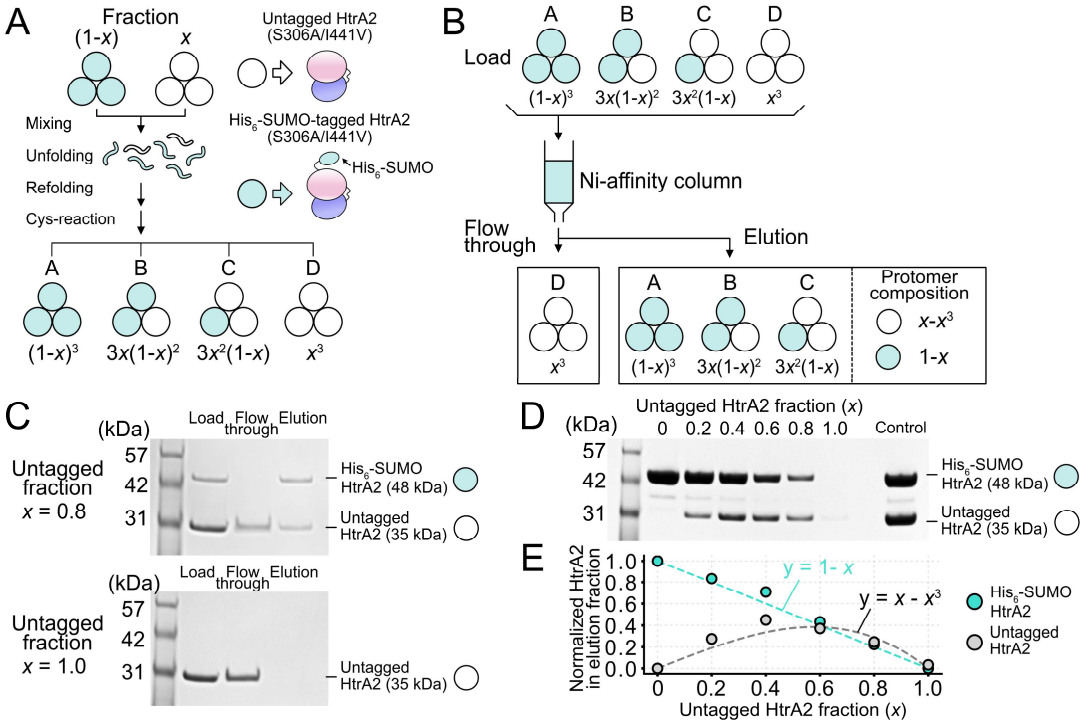

Figure S2. Random mixing of HtrA2 protomers into trimers. (A) To test whether the assembly of asymmetric HtrA2 trimers via the unfolding/refolding procedure used leads to random incorporation of subunits, we prepared mixed HtrA2 protein samples comprised of untagged (white circles) and His_6-SUMO-tagged (light-blue circles) protomers (S306A/I441V mutant) in different ratios, and assessed the distribution of subunits within each particle. The procedure used to prepare mixed HtrA2 trimers is illustrated schematically. The four possible configurations of trimeric HtrA2 (A-D) along with their expected molar fractions are shown below. (B) The mixed proteins were loaded onto a Ni-affinity column; the trimer corresponding to configuration D flows through the Ni-affinity resin, while

configurations A-C are captured by the resin through their His_6-SUMO-tags and subsequently collected in the elution fraction with 300 mM imidazole. The molar fractions of untagged to His_6-SUMO-tagged protomers in the elution fraction can be calculated to be x-x^3 (= $1/3\times3x(1-x)^2+2/3\times3x^2(1-x)$) and $1-x$ (= $(1-x)^3+2/3\times3x(1-x)^2+1/3\times3x^2(1-x)$), respectively, assuming random mixing. (C) (*top*) Proteins mixed at a molar ratio of His_6-SUMO-tagged:untagged = 20%:80% (x = 0.8) were purified via Ni-affinity chromatography and both flow-through and eluant fractions were analyzed by SDS-PAGE. The increased molecular mass of the His_6-SUMO-tagged protomer (~48 kDa) relative to the untagged protomer (~35 kDa) enabled separation of these two species on an SDS-PAGE gel. Both untagged and tagged protomer bands were observed in the elution fraction, showing that untagged protomers co-assembled into trimers containing one or more His_6-SUMO-tag subunits by the refolding procedure. (*bottom*) In the Ni-affinity purification of symmetric untagged proteins (x=1), the untagged protomer band was not observed in the elution fraction, ruling out the possibility of non-specific binding to the resin. (D) SDS-PAGE analyses of the elution fractions of mixed trimers obtained with different His_6-SUMO-tagged:untagged ratios (x = 0, 0.2, 0.4, 0.6, 0.8, and 1.0). In the control lane, equimolar samples comprising His_6-SUMO-tagged and untagged HtrA2 were separated to highlight the differences in band intensities per mole (His_6-SUMO-tagged/non-tagged ~ 1.3). (E) Plot of the relative amount of protomers in the elution fraction (y) as a function of the untagged protomer fraction (x), as estimated from SDS-PAGE band intensities shown in (D). Each band intensity was normalized by the intensity of the corresponding control band (D, right) to account for differences in band intensities for His_6-SUMO-HtrA2 and untagged HtrA2, and then further normalized so that the maximum value of y is 1. Relative amounts of His_6-SUMO-tagged and untagged protomers are indicated by light-blue and black circles, respectively. The expected correlations of His_6-SUMO-tagged protomer (cyan, $y = 1-x$) and untagged protomer (black, $y = x-x^3$) are shown as dotted lines The experimentally obtained profiles are in good agreement with the expected correlations assuming a random incorporation of each protomer-type during the refolding process.

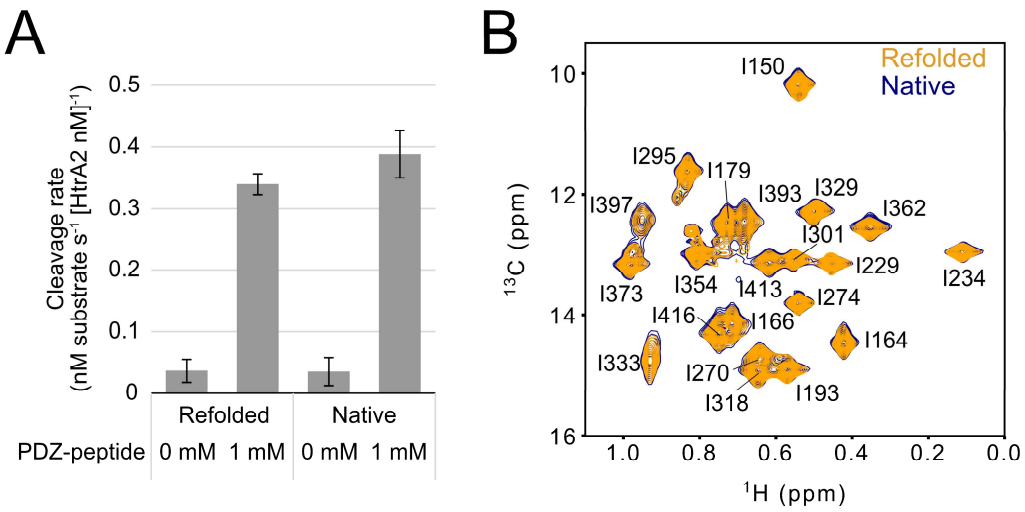

Fig. S3 Unfolding/refolding has no effect on the peptidase activity or the structure of HtrA2. (A) Bar plots of the peptidase activity of refolded (left) and native (right) HtrA2 measured in the presence and absence 1 mM PDZ-peptide. Error bars correspond to 1 SD based on triplicate measurements. (B) Superposition of ^{13}C-^{1}H HMQC spectra of U-^{2}H, *proR* ILVM S306A/I441V prepared with (orange) or without (navy) unfolding/refolding. All NMR data sets were recorded at 23.5 Tesla and 40 °C.

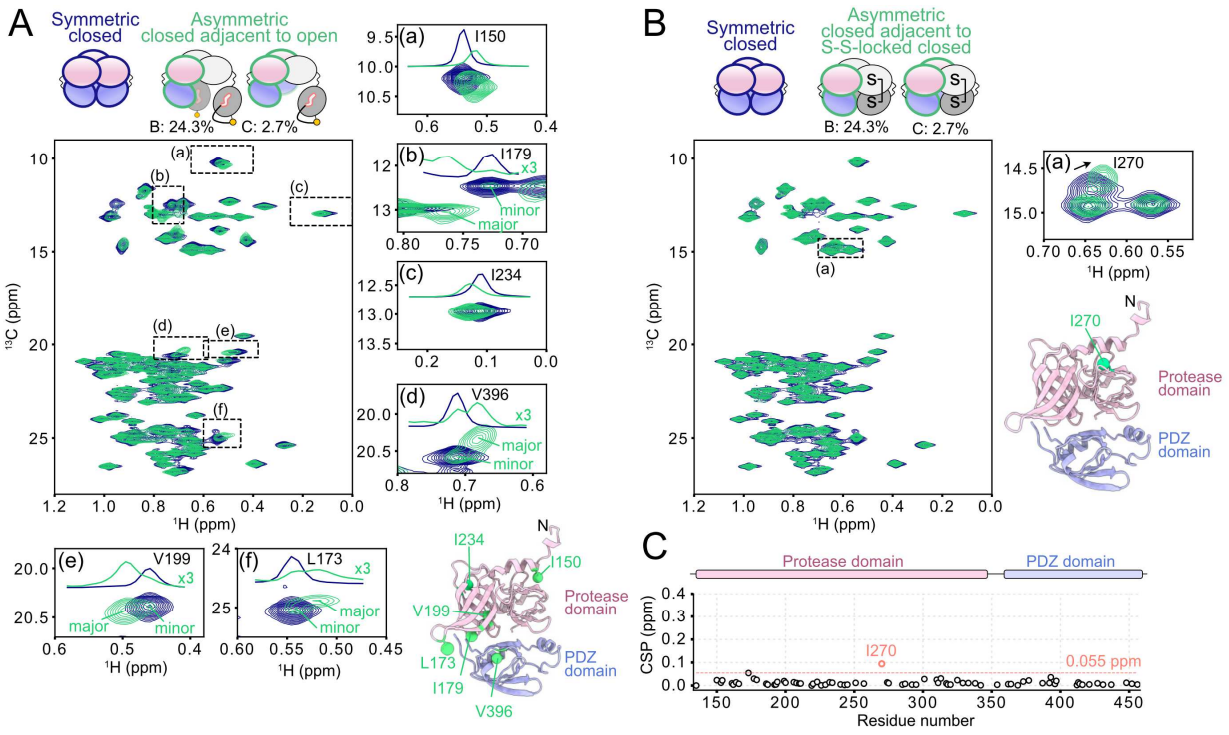

Figure S4. NMR spectra of protomer-mixed HtrA2 samples. (A) Superposition of ^{13}C-^{1}H HMQC spectra of the symmetric U-^{2}H, *proR* ILVM-$^{13}CH_3$ S306A/I441V HtrA2 sample (navy) and the asymmetric HtrA2 sample prepared by mixing 90% U-^{2}H, E425C/S306A/I441V PDZ-peptide stapled/open protomers and 10% U-^{2}H, *proR* ILVM-$^{13}CH_3$ S306A/I441V protomers (green). Enlarged views of (a) I150, (b) I179, (c) I234, (d) V396, (e) V199, and (f) L173 methyl correlations are shown. Major and minor signals are indicated in the enlarged views, most likely corresponding to peaks derived from configurations B and C, respectively, and ^{1}H 1D projections that trace maximum intensities in the displayed regions are also shown. The ^{1}H 1D projections of the spectrum recorded on the asymmetric HtrA2 in (b), (d), (e), and (f) were multiplied by a factor of 3 for ease in visualization. In the bottom right, *proR* ILV methyl carbons of the selected residues are shown as spheres on the HtrA2 protomer structure (from the crystal structure of the HtrA2 trimer, PDB ID: 1LCY). (B) Superposition of ^{13}C-^{1}H HMQC spectra of the symmetric U-^{2}H, *proR* ILVM-$^{13}CH_3$ S306A/I441V HtrA2 sample (navy) and the asymmetric HtrA2 sample prepared by mixing 90% U-^{2}H, Met-$^{13}CH_3$ V226C/Y428C/S306A/I441V S-S locked/closed and 10% U-^{2}H, *proR* ILV-$^{13}CH_3$ S306A/I441V protomers (green). (a) Enlarged view of spectral region focusing on I270, showing a significant CSP (> 0.055 ppm, defined in Fig. 3C) is highlighted. In the bottom right, the δ1 methyl carbon of I270 is shown as a sphere on the HtrA2

protomer structure (from the crystal structure of the HtrA2 trimer, PDB ID: 1LCY). (C) Plot of the CSP values observed in the panel B and defined as in the legend to Figure 3. Schematics of HtrA2 trimeric structures in each sample are shown above the corresponding spectrum. The NMR-active protomers in each sample are colored pink (protease domain) and light-blue (PDZ domain). All NMR data were recorded at 23.5 Tesla and 40 °C.

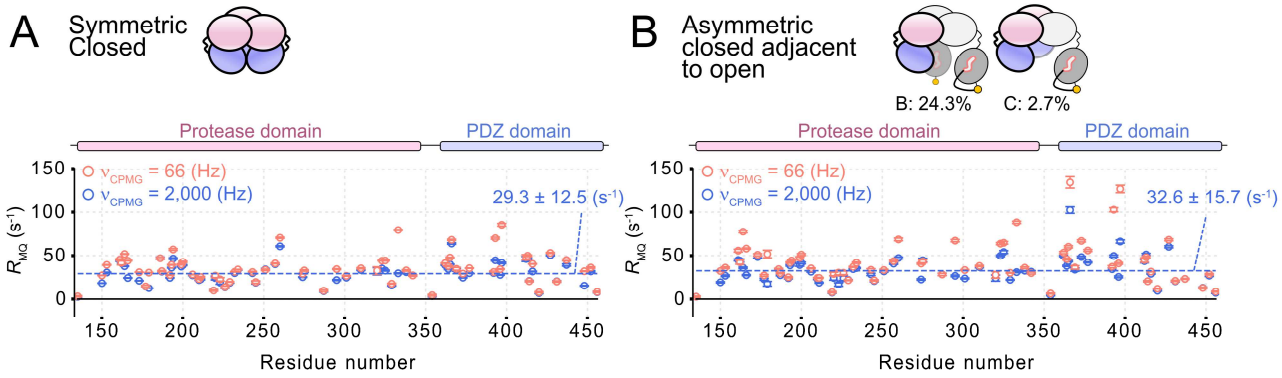

Figure S5. Plots of ^{13}C-^{1}H MQ relaxation rates. Plots of ^{13}C-^{1}H MQ relaxation rates (R_{MQ}) of the symmetric U-^{2}H, *proR* ILVM-$^{13}CH_3$ S306A/I441V HtrA2 sample (A) and the asymmetric HtrA2 sample prepared by mixing 90% U-^{2}H, E425C/S306A/I441V PDZ-peptide stapled/open protomers and 10% U-^{2}H, *proR* ILVM-$^{13}CH_3$ S306A/I441V protomers (B). R_{MQ} rates measured with 66 Hz and 2,000 Hz CPMG fields are shown as red and blue circles, respectively. The mean R_{MQ} rates measured with 2,000 Hz CPMG fields are plotted as blue horizontal dashed lines; mean ± SD values are indicated in the upper right corners of the plots. Structural schematics of HtrA2 trimers in each of the studied samples are shown above the plots. The domains for the NMR-visible protomers are colored pink (protease domain) and light-blue (PDZ domain). All NMR data were recorded at 14.0 Tesla and 40 °C.

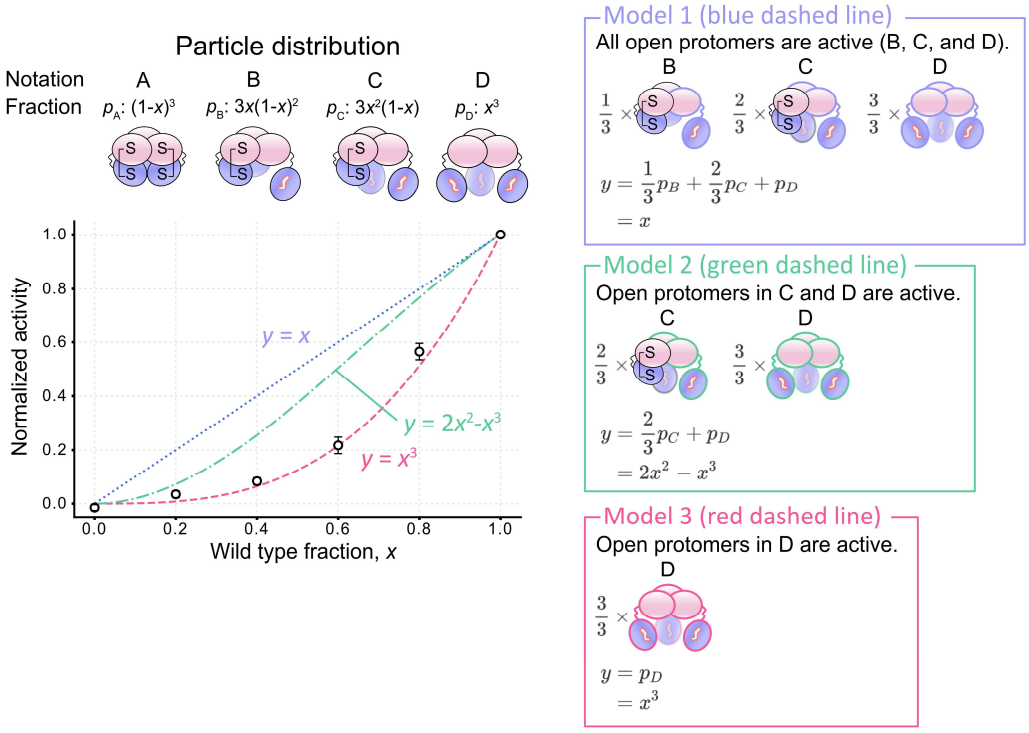

Figure S6. Modeling HtrA2 peptidase activity using mixed samples under oxidizing conditions. (*left*) Plot of normalized peptidase activity (y, white circle) as a function of the molar fraction of wild-type protomers (x). Error bars correspond to 1 SD based on triplicate measurements. The expected normalized activity profiles for the models to the right are shown as colored dotted lines (Model 1 in blue, Model 2 in green, and Model 3 in red), with the appropriate equations relating activity to x indicated. Schematics of the four possible configurations of trimeric HtrA2 (A-D) along with their expected molar fractions from the binomial distribution are shown above the plot. (*right*) Schematics for three different models of HtrA2 activity. The expected relationship between normalized activity and the molar fraction of wild-type protomers is indicated for each case. In Model 1 (blue), all open protomers in configurations B, C, and D are equally active, leading to the $y = x$ relationship. In Model 2 (green), the open protomers in configurations C and D are active, while the open protomer in configuration B is not, leading to the $y = 2x^2-x^3$ relationship. In Model 3 (red), only open protomers in configuration D are active, while the open protomers in configurations B and C are not, leading to the $y = x^3$ relationship. The multiplicative factors of 1/3, 2/3, and 3/3 for p_B, p_C, and p_D account for the number of open protomers in each type of trimeric particle.

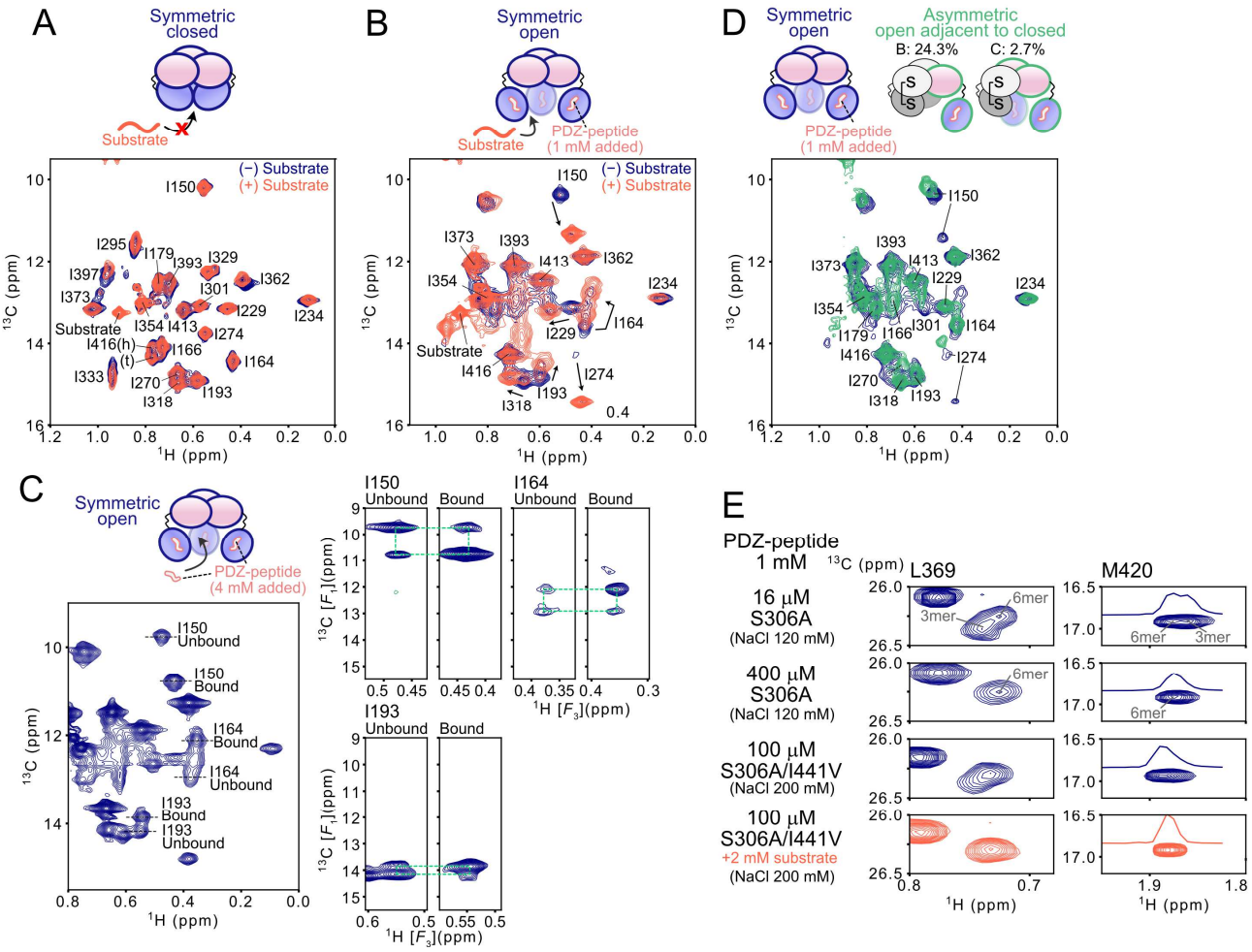

Figure S7. NMR spectra of HtrA2 with substrate and PDZ-peptide. (A) ^{13}C-^{1}H HMQC spectra of U-^{2}H, *proR* ILVM S306A/I441V HtrA2 in the absence (navy) and presence (orange) of 2 mM substrate. Both spectra were recorded in the absence of PDZ-peptide, with 200 mM NaCl added to the buffer. The I416 methyl signals in the hexamer (P_6) and trimer (P_3) states are indicated as (h) and (t), respectively. (B) Superposition of ^{13}C-^{1}H HMQC spectra of U-^{2}H, *proR* ILVM S306A/I441V HtrA2 in the absence (navy) and presence (orange) of 2 mM substrate. Both spectra were recorded in the presence of 200 mM NaCl and 1 mM PDZ-peptide. (C) ^{13}C-^{1}H HSQC spectrum of U-^{2}H, Ileδ1-^{13}CHD$_2$ S306A/I441V HtrA2 in the presence of 4 mM PDZ-peptide. At this high concentration the binding of the PDZ-peptide to the PDZ domain is saturated, and some binding also occurs at the substrate binding site in the protease domain; the resultant populations of open-inactive (no PDZ-peptide in substrate binding site) and active (PDZ-peptide in active site) conformations were ~0.4 and ~0.6, respectively. ^{13}C[F_1]-^{1}H[F_3] strips from

a 3D ^{1}H-^{13}C[t_1]-*mix*-^{13}C[t_2]-^{1}H[t_3] magnetization-exchange experiment (t_{mix} = 900 ms), highlighting selected methyl groups (I150, I164, and I193) exchanging between conformations with and without PDZ-peptide in the substrate binding site are shown to the right. (D) Superposition of ^{13}C-^{1}H HMQC spectra of the symmetric U-^{2}H, *proR* ILVM S306A/I441V HtrA2 sample (navy) and the asymmetric HtrA2 sample prepared by mixing 90% U-^{2}H, Met-$^{13}CH_3$ V226C/Y428C/S306A/I441V S-S locked/closed and 10% U-^{2}H, *proR* ILV-$^{13}CH_3$ S306A/I441V protomers (green), in the presence of 200 mM NaCl and 1 mM PDZ-peptide. A number of peaks from open-inactive and open-active conformations are highlighted (for example, I150 and I274). (E) Selected regions of ^{13}C-^{1}H HMQC spectra of U-^{2}H, *proR* ILVM S306A HtrA2 or U-^{2}H, *proR* ILVM S306A/I441V HtrA2 obtained with different total protein, salt, and substrate concentrations, focusing on L369 and M420 methyl signals. The assignments of the fully-bound trimer (P_3L_3) and hexamer (P_6L_6) are indicated (*top*). All NMR data sets were recorded at 23.5 Tesla and 40 °C. Schematics of trimer structures for each sample in A-D are shown above the spectra.

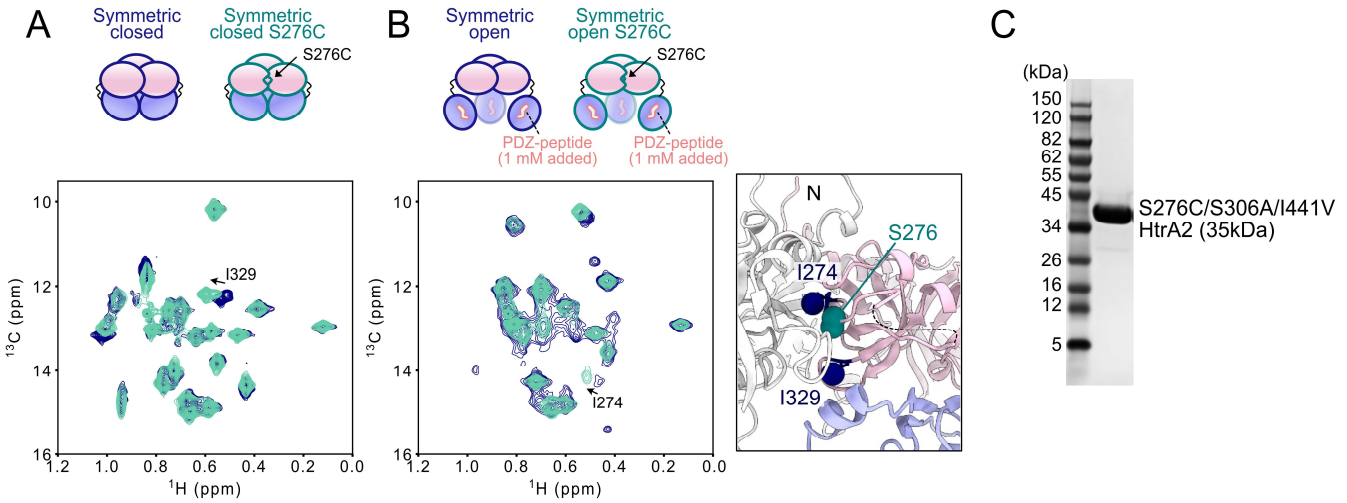

Figure S8. NMR spectra of the S276C disease mutant. (A, B) Superposition of ^{13}C-^{1}H HMQC spectra of U-^{2}H, *proR* ILVM S306A/I441V (navy) and U-^{2}H, ILVM S276C/S306A/I441V HtrA2 (deep green) in the absence (A) and presence (B) of 1 mM PDZ-peptide, with 200 mM NaCl added to the buffer. In the right inset, side-chain heavy atoms of S276 and the Cδ1 carbons of residues I274 and I329, whose methyl groups showed small chemical shift differences in the S276C mutant, are shown as spheres on the HtrA2 trimer structure (PDB ID: 1LCY). The neighboring subunit is colored in gray for visualization. Schematics for each sample are shown on above the spectra. All NMR data were recorded at 23.5 Tesla and 40 °C. (C) SDS-PAGE analysis of the S276C/S306A/I441V mutant HtrA2, showing that the disulfide-linked dimer band was not observed (*i.e.* no inter-protomer crosslinks are formed).

SI References

1. Y. Toyama, R. W. Harkness, T. Y. T. Lee, J. T. Maynes, L. E. Kay, Oligomeric assembly regulating mitochondrial HtrA2 function as examined by methyl-TROSY NMR. *Proc. Natl. Acad. Sci. USA* **118** (2021).

2. V. Tugarinov, V. Kanelis, L. E. Kay, Isotope labeling strategies for the study of high-molecular-weight proteins by solution NMR spectroscopy. *Nat. Protoc.* **1**, 749–754 (2006).

3. P. Gans, *et al.*, Stereospecific Isotopic Labeling of Methyl Groups for NMR Spectroscopic Studies of High-Molecular-Weight Proteins. *Angew. Chem. Int. Ed.* **49**, 1958–1962 (2010).

4. J. Carlsson, H. Drevin, R. Axen, Protein thiolation and reversible protein-protein conjugation. *N*-Succinimidyl 3-(2-pyridyldithio)propionate, a new heterobifunctional reagent. *Biochem. J.* **173**, 723–737 (1978).

5. D. Barthelme, J. Z. Chen, J. Grabenstatter, T. A. Baker, R. T. Sauer, Architecture and assembly of the archaeal Cdc48·20S proteasome. *Proc. Natl. Acad. Sci. USA* **111** (2014).

6. V. Tugarinov, P. M. Hwang, J. E. Ollerenshaw, L. E. Kay, Cross-correlated relaxation enhanced ^{1}H-^{13}C NMR spectroscopy of methyl groups in very high molecular weight proteins and protein complexes. *J. Am. Chem. Soc.* **125**, 10420–8 (2003).

7. L. E. Kay, Artifacts can emerge in spectra recorded with even the simplest of pulse schemes: an HMQC case study. *J. Biomol. NMR* **73**, 423–427 (2019).

8. F. Delaglio, *et al.*, NMRPipe: A multidimensional spectral processing system based on UNIX pipes. *J. Biomol. NMR* **6**, 277–293 (1995).

9. J. J. Helmus, C. P. Jaroniec, Nmrglue: an open source Python package for the analysis of multidimensional NMR data. *J. Biomol. NMR* **55**, 355–367 (2013).

10. C. A. Waudby, A. Ramos, L. D. Cabrita, J. Christodoulou, Two-Dimensional NMR Lineshape Analysis. *Sci. Rep.* **6**, 1–8 (2016).

11. M. W. Maciejewski, *et al.*, NMRbox: A Resource for Biomolecular NMR Computation. *Biophys. J.* **112**, 1529–1534 (2017).

12. D. M. Korzhnev, K. Kloiber, V. Kanelis, V. Tugarinov, L. E. Kay, Probing Slow Dynamics in High Molecular Weight Proteins by Methyl-TROSY NMR Spectroscopy: Application to a 723-Residue Enzyme. *J. Am. Chem. Soc.* **126**, 3964–3973 (2004).

13. N. A. Farrow, O. Zhang, J. D. Forman-Kay, L. E. Kay, A heteronuclear correlation experiment for simultaneous determination of ^{15}N longitudinal decay and chemical exchange rates of systems in slow equilibrium. *J. Biomol. NMR* **4**, 727–734 (1994).

14. E. Rennella, R. Huang, A. Velyvis, L. E. Kay, $^{13}CHD_2$–CEST NMR spectroscopy provides an avenue for studies of conformational exchange in high molecular weight proteins. *J. Biomol. NMR* **63**, 187–199 (2015).

15. L. M. Martins, *et al.*, Binding specificity and regulation of the serine protease and PDZ domains of HtrA2/Omi. *J. Biol. Chem.* **278**, 49417–49427 (2003).